International Journal of Food Science +Technology

International Journal of Food Science and Technology 2023, **58**, 2489–2497

Original article

Microencapsulation of astaxanthin by ionic gelation: effect of different gelling polymers on the carotenoid load, stability and bioaccessibility

Martina Vakarelova,[1] Francesca Zanoni,[1] Giulia Donà,[1] Ilaria Fierri,[2] Roberto Chignola,[2] Sara Gorrieri[2] & Gianni Zoccatelli[2]*

1 Sphera Encapsulation SRL, Villafranca di Verona, Verona 37062, Italy
2 Department of Biotechnology, University of Verona, Verona 37134, Italy

(Received 24 November 2022; Accepted in revised form 27 February 2023)

Summary Astaxanthin (ASX) is a carotenoid characterised by numerous health-promoting properties but biased by scarce chemical stability. Our aim was to microencapsulate ASX through ionic gelation to improve its stability and bioaccessibility, evaluating the performance of low-methoxyl pectin (LMP) and chitosan, besides the most common alginate. Three formulations were tested: 3% pectin (Pec), 3% pectin + chitosan shell (PecChi) and 1.5% alginate—1.5% LMP + chitosan shell. The results showed that chitosan deposited onto PecAlChi and PecChi beads improved particle sphericity and limited oil oxidation during processing. PecAlChi provided the highest encapsulation efficiency (87%) and bioaccessibility (58%). The stability test at 65°C × 24 days showed different polymer-dependent degradation kinetics, with PecChi providing the highest stability (48%). In conclusion, encapsulation performance strongly depended on the chitosan shell and the gelling polymers. This suggests that tuning the alginate/pectin ratio may lead to the best compromise between stability and bioaccessibility.

Keywords Astaxanthin, *Haematococcus pluvialis*, ionic gelation, microencapsulation, simulated gastrointestinal digestion, stability.

Introduction

Astaxanthin (ASX) is a natural ketocarotenoid (3,3′-dihydroxy-β-β'-carotene-4,4′-dione) present in many marine and aquatic organisms. Unlike carotenes, it has a polar region at either end of the ionone rings that provide the structure with a partially amphiphilic nature so that it fits precisely into the cell membrane bilayer (McNulty *et al*., 2007). This characteristic gives ASX extraordinary antioxidant capacity (Miki, 1991; Shimidzu *et al*., 1996; Kobayashi & Sakamoto, 1999), exerted by different mechanisms like singlet oxygen quenching and free radical scavenging. The antioxidant properties of ASX may play an essential role in protecting against pathological conditions like inflammation, cancer, ageing and macular degeneration, or enhancing the immune response, liver function, skin and cardiovascular health (Shah *et al*., 2016; Fakhri *et al*., 2018; Simat *et al*., 2022). For these reasons, ASX is currently being investigated as a potential compound for producing functional foods and supplements with improved benefits for human health.

The most common source of ASX is the green microalgae *Haematococcus pluvialis* (*H.p.*), capable of reaching up to 5% ASX on dry weight (Khoo *et al*., 2019). Krill (Xie *et al*., 2019) and by-products deriving from the processing of crustaceans (Simat *et al*., 2022) represent other sustainable sources.

Natural ASX occurs as a mixture of mono- or di-esters with fatty acids. Depending on the pattern of esterification, the stability and the bioavailability are different (Yang *et al*., 2021). In addition, while for carotenoids, the all-trans form is generally considered the most bioactive form, in the case of ASX, there is evidence that the cis forms, originated from physical/chemical stress, possess superior antioxidant capacity (Liu & Osawa, 2007).

The intrinsic susceptibility to degradation mediated by temperature, oxygen, light and extreme pHs (Ambati *et al*., 2014) limits food and nutraceutical applications of ASX. For this reason, different micro- and nano-encapsulation approaches have been proposed to improve the stability of ASX, i.e. emulsions

*Correspondent: E-mail: gianni.zoccatelli@univr.it

doi:10.1111/ijfs.16389

(Khalid *et al.*, 2017), liposomes (Chiu *et al.*, 2016), lipid nanoparticles (Rodriguez-Ruiz *et al.*, 2018), solvent evaporation (Zanoni *et al.*, 2019; Binatti *et al.*, 2021), spray-drying (Pu *et al.*, 2011; Bustos-Garza *et al.*, 2013) and ionic (or ionotropic) gelation (Lee *et al.*, 2011; Lin *et al.*, 2016; Vakarelova *et al.*, 2017; Zhang *et al.*, 2017; Niizawa *et al.*, 2019). In particular, ionic gelation (IG) represents a promising technique to microencapsulate ASX-containing oils and oleoresins. The main advantages of this approach are the high oil encapsulation efficiency (Chan, 2011), the possibility to employ GRAS (generally recognised as safe) wall materials and the low operating temperatures that help prevent carotenoid degradation. In all studies dealing with IG, ASX was encapsulated using alginate cross-linked with bivalent calcium ions, even though in a previous study, we showed that ASX could be encapsulated also in low methoxyl pectin (LMP) (Vakarelova *et al.*, 2017). The rationale for using LMP, is that, similarly to alginate, it possesses a relevant percentage of carboxyl groups that can be coordinated by calcium ions to form egg-box-based gel structures. In agreement with another study (Chan, 2011), we showed that alginate was characterised by considerable oil loss (4.3%) during drying despite its excellent encapsulation aptitude. LMP, on the contrary, displayed much lowers oil losses (0.3%) and it is worth noting that this polysaccharide also represents a more sustainable material since it derives from by-products of citrus fruit processing. Knowing the superior capacity of LMP in limiting the loss of oil during encapsulation, in the present work, we sought to investigate further the effect of using alginate and LMP as gelling polymers and the role of another important sustainable polymer, i.e. chitosan, as additional protective shell material on important quality traits like loading capacity, thermal stability and the bioaccessibility of encapsulated ASX.

Materials and methods

Materials

Dried *H.p.* cells were provided by AlgainEnergy S.r.l. Soybean oil was purchased in a local market. Na-alginate was obtained from Merck KGaA (Darmstadt, Germany, code W201502), food-grade low-methoxyl pectin from *citrus* fruits was from Silva Extracts (Bergamo, Italy). Pectin was characterised by 25–35% degree of methylation and 20–25% degree of amidation. Chitosan (deacetylation degree: >90%; molecular weight: 240–810 kDa) was provided by Giusto Faravelli S.p.a. (Milano, Italy). A commercially available food-grade soybean oil (Valsoia, Italy) was used to solubilise *H.p.* oleoresin. Ethyl acetate, hydrochloric acid, n-hexane, isooctane, calcium chloride dihydrate, potassium iodide, sodium thiosulphate and p-anisidine were purchased from Merck KGaA.

Algae extraction

H.p. oleoresin was extracted using a previously described protocol with some modifications (Bustos-Garza *et al.*, 2013). Five grams of dry algae powder were mixed with 1 mL of 3 M HCl and treated in a microwave oven for 1 min at 100 W. The pretreated algae were extracted with 25 mL of ethyl acetate in a glass tube for 60 min under agitation at 50 °C. The solid part was separated by centrifugation at 3500 ***g*** for 10 min and discarded. The oleoresin was dried by a rotary evaporator (Buchi, Flawil, Switzerland) at 35 °C and 10 kPa until the oleoresin weight remained constant. The dried material was kept in the dark at 4 °C until use.

Spectrophotometric analysis

Quantification of astaxanthin was carried out by a UV/VIS spectrophotometer (Unicam UV2). The samples were diluted in ethyl acetate and the absorbance was measured at 480 nm. ASX concentration [ASX], expressed as mg/mL, was calculated with the following equation (Vakarelova *et al.*, 2017):

$$[\mathrm{ASX}] = \frac{10 \times A_{480}\ \mathrm{x\ DF}}{E_{(1\%;\,1\ \mathrm{cm})} \times d} \qquad (1)$$

where A_{480} is the absorbance at 480 nm; DF the dilution factor; $E_{(1\%;1\mathrm{cm})}$: ASX specific absorbance (2150 g^{-1} L cm^{-1}); d the optical path (1 cm).

Encapsulation

Pectin and Na-alginate were used for the encapsulation of ASX-enriched oil. These polysaccharides form gels in the presence of divalent cations (e.g. Ca^{2+}). Three different formulations were studied: (i) 3% Pectin (Pec), (ii) 3% pectin surrounded by a chitosan shell (PecChi) and (iii) 1.5% pectin-1.5% alginate surrounded by a chitosan shell (PecAlChi). The polymers were dispersed overnight in distilled water under gentle stirring at room temperature to allow their rehydration. Oleoresin was solubilised in soybean oil (ASX-enriched oil), leading ASX final concentration to be 1.3 mg g^{-1} and combined with the polymer solutions at a polymer:oleoresin ratio of 6:1 (w:w) as described in our previous study (Vakarelova *et al.*, 2017). Smaller or greater ratios, in our experience, give either too soft or too much diluted (in terms of payload) beads. Finally, the mixture was emulsified using an Ultra-Turrax homogeniser (IKA-Werke, Staufen, Germany) at 13 000 rpm for 5 min at room temperature. The emulsion was dripped using a 0.6 mm-diameter needle in the gelling solution consisting of 1%

acetic acid, 0.2 M $CaCl_2$, eventually containing 1% chitosan (Primex, Siglufjordur, Iceland) to provide the additional shell. The distance between the needle and the surface of the gelling solution was set at 10 cm. The beads were left to stir for 1 h to allow the polymers in the solution to best interact with calcium ions and chitosan. The beads were washed with distilled water to eliminate excess calcium and dried. Drying was achieved by a Mini-Glatt fluid bed reactor (Glatt, Binzen, Germany) with an airflow of 20 $m^3\ h^{-1}$ for 90 min. This parameter allowed for the best fluidisation of the beads inside the reactor. The process was conducted at 35 °C, similar to what we described previously (Menin *et al.*, 2018), to limit the oxidation of ASX.

Moisture content and water activity (aw)

Moisture content was assessed gravimetrically following the AOAC 925.09 standard method (AOAC, 2016). Water activity was measured using an HC2AW instrument (Rotronic, Rho, Milano, Switzerland) at 25 °C. All analyses were carried out in triplicate.

Morphology

The size and morphology of the beads were evaluated by a Leica EZ4W stereo microscope (Leica Microsystems, Milan, Italy). The distributions of the measured diameters were estimated using a smooth kernel density algorithm implemented in the software Mathematica v. 11.2.0.0 (Wolfram Research, Inc., Champaign, IL, USA) using the least square cross-validation method for bandwidth selection. The analyses showed that approximately 50 beads were sufficient to obtain smooth estimated probability density functions (i.e. distributions with no irregular peaks). The sphericity factor (SF) of the beads was calculated as previously reported (Chan *et al.*, 2009) using the following equation:

$$\mathrm{SF} = \frac{(D\mathrm{max} - D\mathrm{per})}{(D\mathrm{max} + D\mathrm{per})} \tag{2}$$

where Dmax is the maximum diameter passing through the centroid of the bead and Dper the diameter perpendicular to Dmax. A SF = 0 is expected for a perfectly spherical shape, while SF > 0 values indicate a departure from perfect sphericity. A SF < 0.05 is considered acceptable.

Oil extraction from the beads

Encapsulation efficiency and payload

A batch of beads obtained from 7 g of the emulsion was incubated with 10 mL of a 100 mM Na phosphate buffer, 50 mM NaCl, pH 7.4 and left in agitation until the beads were completely disrupted. Twenty millilitres of ethyl acetate were added, and the samples were left under stirring for 1 h and finally centrifuged at 10 000 ***g*** for 10 min. ASX concentration was determined spectrophotometrically, and the efficiency was calculated using the following formula (Niizawa *et al.*, 2019):

$$\mathrm{EE}\% = \frac{Ae}{Ao} \times 100 \tag{3}$$

where A_e is the amount of extracted astaxanthin, and A_o the amount of astaxanthin present in 1 g of enriched oil used to prepare the emulsion according to the ratio 1:6. Ethyl acetate was then removed by a rotary evaporator, and the oil residue (total extractable oil, TEO) was weighed.

The payload of the beads (i.e. the mg of ASX available in 1 g of encapsulated product) was calculated as follows:

$$\mathrm{Payload} = \frac{\mathrm{Ae\ (mg)}}{\mathrm{weight\ of\ the\ beads\ (g)}} \tag{4}$$

Surface oil

The measurement of the surface oil (SO) was carried out following the protocol proposed by Liu *et al.* (2010) with minor modifications. An amount of 0.5 g of beads was dispersed in 20 mL of hexane and left to stir vigorously for 30 s. The extract was filtered to eliminate the microcapsules, and hexane was eliminated by a rotary evaporator. The oil residue (SO) was weighted, and the SO% was calculated as follows:

$$\mathrm{SO}\% = \frac{\mathrm{SO\ (g)}}{\mathrm{TEO\ (g)}} \times 100 \tag{5}$$

Determination of the degree of lipid oxidation

The degree of oxidation of astaxanthin-enriched oil before and after the encapsulation was determined to evaluate whether the process, even though it is considered a delicate process, could have deteriorated the quality of the oil by promoting oxidation reactions.

Peroxide value

The peroxide value (PV) was calculated by iodometric titration following the official method AOCS Cd 8–53 (AOCS, 2003) with some modifications. About 0.5 g of TEO were placed in a glass tube and diluted in 15 mL of an acetic acid:iso-octane (3:2) mixture. After the addition of 0.5 mL of saturated potassium iodide, the sample was shaken for 1 min. Deionised water (15 mL) and gelatinised starch (0.5 mL of a 1% w:v solution) were added, and iodine titration was carried out with a 0.001 N sodium thiosulfate solution

(Vetrotecnica, Padova, Italy). The peroxide value was expressed as milliequivalents of O_2 (mEq O_2) per kg using the following formula:

$$\mathrm{PV}\left(\frac{\mathrm{mEqO_2}}{\mathrm{kg}}\right) = \frac{\mathrm{N\ titratant} \times \mathrm{V\ titratant} \times 1000}{\mathrm{Oil\ weight\ (g)}} \quad (6)$$

where N and V are the normality and the volume of the titrant (sodium thiosulfate) respectively.

p-anisidine value

The AOCS Official Method Cd 18–90 (AOCS, 2009) was employed. About 0.5 g of TEO were diluted in 10 mL of iso-octane. A volume of 2.5 mL was combined with 0.5 mL of *p*-anisidine 0.25% w/v and allowed to react for 10 min in dark conditions. The absorbance of the solutions before (Ai) and after (Af) the reaction with *p*-anisidine was determined at a wavelength of 350 nm. The *p*-anisidine value was then calculated using the following formula:

$$\mathrm{AV} = \frac{V \times (1.2 \times Af - Ai)}{\mathrm{Oil\ weight}\ (g)} \quad (7)$$

where V is the volume of iso-octane.

Thermal stability test

Samples of the three formulations were subjected to a thermal treatment to accelerate ASX degradation as previously proposed (Leong *et al.*, 2016). Amounts of 0.5 g of dry beads were placed in 50 mL falcon tubes, flushed with nitrogen, sealed, covered with aluminium and incubated at 65 °C for 6, 12, 18 and 24 days. The stability assessment was carried out by measuring the amount of ASX remaining inside the beads as described in Section 2.7.1, and normalising these data on the ASX amount at the time zero. The experiments were performed in triplicate.

Simulated gastrointestinal digestion of the beads

The simulated gastrointestinal digestion was carried out following a previously published method (Yi *et al.*, 2015) with some modifications. An amount of 250 mg of dry beads was placed in a glass tube containing 4 mL of simulated gastric fluids (SGF: 50 mM NaCl, 0.084 M HCl, porcine pepsin 1 mg/mL) and kept under agitation at 37 °C. After 60 min, the passage to the intestinal phase started with the addition of 4 mL of simulated intestinal fluids (SIF: 0.1 M sodium phosphate buffer, 50 mM NaCl, pancreatin from porcine pancreas 2 mg/mL) and adjusting the pH with a 1 M NaOH solution until a value of 7.3 was obtained. The samples at the end of the gastric phase and after 60, 120 and 180 min of the intestinal phase were centrifuged at 10000 ***g*** for 20 min, and the supernatants were collected. These were extracted with two volumes of ethyl acetate for 1 h in the dark under continuous agitation. The samples were centrifuged at 10 000 ***g*** for 10 min, and the supernatants were collected. The release of ASX was measured by spectrophotometry as described above.

Statistics

Statistical analyses were performed using SigmaPlot version 12.5 (Systat Software Inc., San Jose, CA, USA) and the data was expressed as mean ± standard deviation. Differences between the experimental groups were assessed using unpaired Student's *t*-test or, where appropriate, by one-way analysis of variance (ANOVA), followed by the *post hoc* Tukey test.

Results and discussion

Physical and morphological characterisation of the beads

In this work, astaxanthin-rich oleoresin from *H.p.* was solubilised in soybean oil and microencapsulated through an IG process using three combinations of polysaccharides. The microbeads were dried with a fluidised bed reactor. In comparison to passive air-drying, fluid bed technology represents a better solution for drying hydrogel microbeads as in a few hours, it is possible to reach a water activity value of about 0.2–0.25. At these values, lipid oxidation, which represents the most deleterious phenomenon affecting food lipophilic molecules such as carotenoids, is considered to proceed at the slowest rate (Velasco *et al.*, 2003). On the contrary, in a previous work, we observed that 24–48 h is necessary to obtain similar water activity values by passive air-drying at room temperature, with the possibility of observing oxidation damages (Menin *et al.*, 2018). The three formulations did not show significant differences in terms of water activity and water content (Table 1).

The SF is a parameter that is frequently used to describe the degree of sphericity of hydrogel beads. Spherical beads are preferred to irregular ones since a seamless shape is generally associated with greater ease of manipulation besides being aesthetically more acceptable by the consumers. Typically, beads/capsules with a SF ≤0.05 can be considered spherical (Chan *et al.*, 2009). As experienced in our previous study (Vakarelova *et al.*, 2017), pectin beads were characterised by low sphericity giving, on average a SF of 0.113. Pure alginate solutions typically give SF <0.05 (Vakarelova *et al.*, 2017). This behaviour is well-known and is independent of the loaded molecules. Indeed, also the encapsulation of folic acid, a water-soluble vitamin, produced beads with lower sphericity when compared to alginate (Madziva *et al.*, 2005). This seems to be due to a faster and more ordered

Table 1 Physical and morphological characteristics of the beads

Carrier	SF	Diameter (μm)	A_w	Water content (%)
Pec	0.113 ± 0.094 a	211 ± 35 a	0.232 ± 0.03 a	4.10 ± 0.13 a
PecChi	0.051 ± 0.028 b	178 ± 15 b	0.222 ± 0.01 a	3.83 ± 0.11 a
PecAlChi	0.054 ± 0.029 b	193 ± 17 ab	0.223 ± 0.03 a	3.75 ± 0.21 a

Values are expressed as mean ± standard deviation. Different letters within each column indicate significant differences ($P \leq 0.05$).
Abbreviations: Aw, water activity; SF, sphericity factor.

cross-linking of alginate than pectin with higher molecular alignment (Pillay & Fassihi, 1999a). Interestingly, our results show that the chitosan shell seems to improve the sphericity of the beads: in fact, PecChi beads were characterised by lower SF (0.051) than Pec samples ($P < 0.05$), thus similar to PecAlChi (0.054). This is also evident observing Fig. 1. This phenomenon might be caused by the electrostatic interaction between the amino groups of chitosan and the anionic polymers contrasting the collapsing of the beads and the shrinkage upon drying (Pillay & Fassihi, 1999a). PecChi samples also showed a significantly smaller average diameter than Pec beads, probably because of the same electrostatic interaction. In the PecAlChi samples, the lower SF than Pec samples is probably due to a combined effect of chitosan and alginate. Previously reported data did not show significant differences in the size of chitosan-coated alginate beads using different concentrations of the two colloids (Taksima *et al.*, 2015). However, in those trials, an uncoated sample was missing, so it is impossible to infer whether even small concentrations of chitosan may affect the morphology of the resulting beads.

Encapsulation efficiency, surface oil and payload

In this study, the EE% was expressed as the ratio between the concentration of extractable ASX and the concentration of the carotenoid theoretically present in the beads, as described by Lee *et al.* (2011). For other encapsulation processes, *e.g.* spray drying, the EE% is often quantified as the difference between total and surface ASX normalised on total ASX (Zhao *et al.*, 2019). This last approach does not consider the amount of entrapped carotenoid that is virtually unextractable. Table 2 shows how the beads containing alginate are characterised by the highest EE%, reaching, on average, a value of 87%. This value is not far from what Lin *et al.* (2016) calculated using alginate. The results also indicate that the presence of the chitosan shell does not hinder the release of the carotenoid. The lower EE% showed by pectin-based beads (62–65%) is probably due to the differences in the polymeric network established by the colloids that interfere with the release of the loaded carotenoid. Similar results were achieved by Arab *et al.* (2019) using a blend of alginate and high methoxyl pectin to encapsulate canthaxanthin. Also, hydrophilic molecules like folic acid showed a similar behaviour: the release from mixed alginate-pectin microparticles of the target molecules was directly correlated with the concentration of alginate (Madziva *et al.*, 2005). The percentage of surface oil (SO%) represents an important parameter as it is supposed to be most susceptible to oxidation (Velasco *et al.*, 2003). The presence of the chitosan shell significantly lowered the values of SO% from 1.93% to 1.67% for pectin beads. The SO% of PecAlChi beads was comparable to that of PecChi samples,

Figure 1 Physical appearance of the dry beads of Pec (a), PecChi (b) and PecAlChi (c).

Table 2 Loading characteristics of the beads

Formulation	EE%	SO%	Payload (mg ASX g^{-1})
Pec	62.48 ± 2.19 a	1.93 ± 0.02 a	0.69 ± 0.002 a
PecChi	65.50 ± 1.98 a	1.67 ± 0.05 b	0.73 ± 0.01 b
PecAlChi	87.43 ± 5.95 b	1.59 ± 0.11 b	0.98 ± 0.06 c

Values are expressed as mean ± standard deviation of three independent experiments. Different letters within each column indicate significant differences ($P \leq 0.05$).
Abbreviations: EE%, encapsulation efficiency; SO%, surface oil.

despite the two formulations showed significantly different EE% (87.43 ± 5.95% vs 65.5 ± 0.9%). This suggests that the shell rather than the polymer composition of the beads matrix determines the amount of SO, hindering its release on the surface of the beads. It could be interesting to evaluate in future the thickness of chitosan deposition on the different gelling materials and whether this could influence the EE% but also other features like the stability of the encapsulated active molecules towards different stress conditions. These results indicate that PecAlChi, characterised by the highest EE% and the lowest SO%, represents the most promising formulation.

Lipid oxidation

We previously showed that even though IG is recognised as one of the mildest encapsulation approaches, to a limited extent, it can induce lipid oxidation, a radical-based reaction that brings to the degradation of unsaturated fatty acids with the onset of off-flavours (Menin *et al.*, 2018). For this reason, we measured primary oxidation products, *i.e.*, peroxides, through peroxide value (PV) and secondary products (aldehydes), by *p*-anisidine value (p-AV) raising upon ASX encapsulation process. Oils presenting PV values greater than 10 mmEq O_2 kg^{-1} are generally considered highly oxidised and low-quality (Negash *et al.*, 2019).

ASX extraction from *H.p.* led to an increase in the oil peroxide value, bringing it to an average value of 4.38 mmEq O_2 kg^{-1} (Table 3). The emulsification and the drying steps represent the most critical point affecting oil oxidation since they intensively expose the unsaturated fatty acids to oxygen. In accordance with the SO% data (Table 2), the oil extracted from Pec beads showed a PV of 9.20 mmEq O_2 kg^{-1} (therefore just below the limit). In contrast, the chitosan-coated beads displayed significantly lower PV values, indicating that chitosan did provide protection against oxidation during processing. Interestingly, no differences were found between PecChi and PecAlChi beads, confirming the hypothesis that the shell, rather than the matrix polymers, affects the susceptibility to oxidation.

Table 3 Lipid oxidation markers

Sample	PV (mEq O_2 kg^{-1})	p-AV
Oil	2.87 ± 0.03 a	3.82 ± 0.05 a
ASX-enriched oil	4.38 ± 0.11 b	4.45 ± 0.10 b
Pec	9.20 ± 0.14 c	5.73 ± 0.17 c
PecChi	6.01 ± 0.08 d	4.24 ± 0.12 b
PecAlChi	5.96 ± 0.02 d	4.63 ± 0.06 b

Different letters within each column indicate significant differences ($P \leq 0.05$). Values are expressed as mean ± standard deviation of three independent experiments.
Abbreviations: p-aV, p-anisidine value; PV, peroxide value.

Therefore, the addition of chitosan was crucial to increase the oxidative stability of the oil without influencing the ASX extraction efficiency, as described above.

p-AV represents an estimate of the secondary oxidation products, particularly alkenals, present in oxidised oils. These compounds are more stable than primary products that, being volatile, are responsible for the perception of rancid odour. As expected, p-AV increased following the production of peroxides as they are formed by the decomposition of these molecules. High p-AV is an indication of a very advanced state of oxidation. In agreement with the data about PV, Pec beads showed the highest values (5.73), thus demonstrating a higher overall degree of oxidation than PecChi and PecAlChi formulations, which showed values of 4.24 and 4.63, respectively (Table 3).

Thermal stability of encapsulated astaxanthin

One of the objectives of this work was to verify whether encapsulation could enhance the stability of ASX. For this reason, we performed a stress test at 65°C to accelerate ASX degradation and verify which formulation could provide the best protection to the carotenoid (Fig. 2). As expected, the unencapsulated oil sample was characterised by a drastic decrease of ASX that became undetectable after the second sampling time (12 days). The degradation kinetics of the encapsulated samples showed different trends. Indeed, while the degradation of PecChi samples displayed a zero-order kinetics ($R^2 = 0.915$; $P < 0.05$) and the best performance in terms of ASX retainment (48% after 24 days), the degradation of ASX in Pec and PecAlChi samples was faster and characterised by a two-slopes profile, of which only the second part obeyed a zero-order kinetics ($P < 0.05$). This particular pattern has already been described (Desobry *et al.*, 1997; Tonon *et al.*, 2010) and is probably due to the fast degradation of non-encapsulated or partially encapsulated ASX located on the boundary of the particles or more in contact with the oxygen present in the pores,

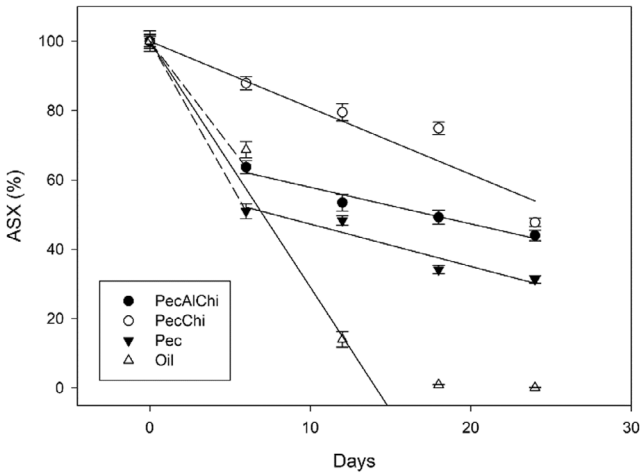

Figure 2 ASX retainment during the accelerated storage test at 65°C for 24 days of Pec, PecChi, PecAlChi and ASX-enriched oil. Straight lines represent the best fittings of the experimental data for each sample. ASX retainment was calculated as the ratio between the extractable ASX at a given time point and the time zero point.

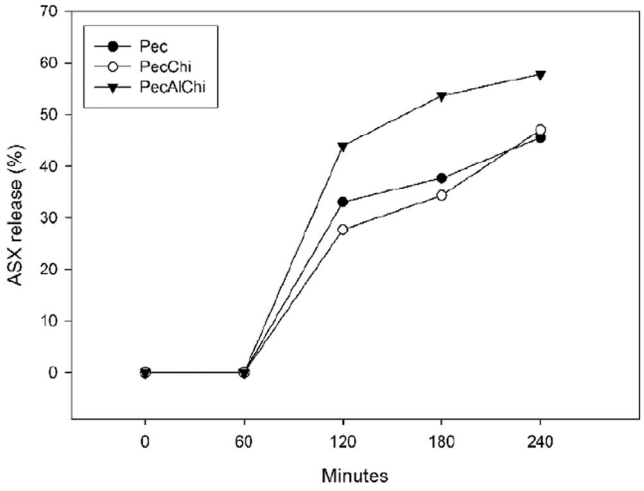

Figure 3 ASX release (bioaccessibility) during simulated gastrointestinal digestion. Gastric phase: 0–60 min; intestinal phase: 60–240 min.

followed by a slower degradation of the internal and less accessible ASX. It is possible that the modification of the cross-linked polymeric network induced by the interaction between pectin and alginate, which allowed for better extraction of ASX (see Table 2), might also be responsible for its faster degradation compared to PecChi. Previous stability studies conducted at 50 °C on alginate-encapsulated ASX showed lower stability (35% retained ASX in 21 days), thus confirming that pectin might contribute better to the protection of the carotenoid (Zhang *et al.*, 2017). These data demonstrate that applying a chitosan shell helps improve ASX stability, which is particularly evident by comparing Pec and PecChi samples. In the case of PecAlChi, the protective effect of chitosan might have been less efficacious due to the presence of alginate, as mentioned above.

Simulated gastrointestinal digestion

To evaluate the ASX bioaccessibility of the three formulations, we employed a simulated gastrointestinal digestion method. To allow a better comparison of the results, the calculated values of released ASX were normalised on each formulation's payload, representing the maximum achievable ASX obtainable from the beads. The results are presented in Fig. 3. As expected, no release of ASX was observed during the gastric phase since the acidic pH promotes the shrinkage of alginate and pectin cross-linked gels (Pillay & Fassihi, 1999b). On the contrary, during the intestinal phase, a time-dependent release of ASX was observed due to different pH and osmolarity conditions that led to a rapid disruption of the egg-box structures. In this case, the chitosan shell did not influence the release of ASX since Pec and PecChi samples showed a similar release. One explanation for this phenomenon may be that chitosan, being soluble at acidic pH, could be dissolved during the gastric phase. Beads containing alginate reached a release of astaxanthin of 58% at the end of digestion, while both those composed of pectin stopped around 46–48%. This result agrees with the EE values presented in Table 2. The higher release displayed by the beads containing alginate depends on the fact that this polymer might establish weaker interaction with ASX or that the matrix structure is less tight, thus favouring the release of the carotenoid.

Conclusions

Three formulations composed of different combinations of polymers were used to encapsulate an ASX-enriched oil by IG. The results indicate that the application of a chitosan shell represents a successful solution to improve the morphology and stability of the ASX-containing beads encapsulated in an LMP matrix (PecChi). On the other hand, the combination of alginate and LMP showed a higher EE and bioaccessibility than LMP. Therefore, from our data and considering the literature about the encapsulation of other bioactive molecules, we can hypothesise a scenario in which alginate and LMP differently affect encapsulation performance depending on their relative abundance: the higher the concentration of pectin, the greater the stability of the carotenoid but the lower its bioaccessibility. On the contrary, alginate would play the opposite role. In this view, the ratio of the two polymers should be carefully evaluated to identify the

best compromise between the stability and bioaccessibility of astaxanthin.

Acknowledgments

Open Access Funding provided by Universita degli Studi di Verona within the CRUI-CARE Agreement.

Author contributions

Martina Vakarelova: Conceptualization (lead); data curation (equal); investigation (lead); project administration (equal). **Francesca Zanoni:** Conceptualization (supporting); data curation (equal); visualization (equal). **Giulia Donà:** Investigation (equal); supervision (supporting). **Ilaria Fierri:** Investigation (equal). **Roberto Chignola:** Data curation (equal); formal analysis (equal); writing – review and editing (equal). **Sara Gorrieri:** Investigation (equal). **Gianni Zoccatelli:** Funding acquisition (lead); project administration (equal); supervision (equal); writing – original draft (lead).

Funding information

This work was supported by the University of Verona (Joint project 2012) and by the Regione del Veneto (code 1695/101/7/1148/2013).

Conflict of interest

The authors have no conflicts of interest to declare.

Ethical review

This study does not involve any human or animal testing.

Data availability statement

Data are available on request from the authors.

References

Ambati, R.R., Phang, S.M., Ravi, S. & Aswathanarayana, R.G. (2014). Astaxanthin: sources, extraction, stability, biological activities and its commercial applications-a review. *Marine Drugs*, **12**, 128–152.

AOAC (2016). *Official method 925.09 Solids (total) and moisture in flour*, 20th ed. Washington, DC: Association of Official Analytical Chemists (AOAC).

AOCS (2003). *AOCS Official Methods and Recommended Practices of the AOCS*. Champaign, IL: AOCS Press.

AOCS (2009). *AOCS Official Methods and Recommended Practices of the AOCS*. Champaign, IL: AOCS Press.

Arab, M., Hosseini, S.M., Nayebzadeh, K. *et al.* (2019). Microencapsulation of microbial canthaxanthin with alginate and high methoxyl pectin and evaluation the release properties in neutral and acidic condition. *International Journal of Biological Macromolecules*, **121**, 691–698. In this publication, the Authors describe the encapsulation of canthaxanthin, a carotenoid close to astaxanthin, using alginate and alginate-high methoxyl pectin as gelling polymers. In agreement with our findings, they showed that alginate-pectin beads were characterized by lower carotenoid release than alginate.

Binatti, E., Zoccatelli, G., Zanoni, F., Donà, G., Mainente, F. & Chignola, R. (2021). Phagocytosis of astaxanthin-loaded microparticles modulates TGFβ production and intracellular ROS levels in J774A.1 macrophages. *Marine Drugs*, **19**, 1–16.

Bustos-Garza, C., Yanez-Fernandez, J. & Barragan-Huerta, B.E. (2013). Thermal and pH stability of spray-dried encapsulated astaxanthin oleoresin from *Haematococcus pluvialis* using several encapsulation wall materials. *Food Research International*, **54**, 641–649.

Chan, E.S. (2011). Preparation of Ca-alginate beads containing high oil content: influence of process variables on encapsulation efficiency and bead properties. *Carbohydrate Polymers*, **84**, 1267–1275.

Chan, E.S., Lee, B.B., Ravindra, P. & Poncelet, D. (2009). Prediction models for shape and size of ca-alginate macrobeads produced through extrusion-dripping method. *Journal of Colloid and Interface Science*, **338**, 63–72.

Chiu, C.H., Chang, C.C., Lin, S.T., Chyau, C.C. & Peng, R.Y. (2016). Improved hepatoprotective effect of liposome-encapsulated astaxanthin in lipopolysaccharide-induced acute hepatotoxicity. *International Journal of Molecular Sciences*, **17**, 1–17.

Desobry, S.A., Netto, F.M. & Labuza, T.P. (1997). Comparison of spray-drying, drum-drying and freeze-drying for beta-carotene encapsulation and preservation. *Journal of Food Science*, **62**, 1158–1162.

Fakhri, S., Abbaszadeh, F., Dargahi, L. & Jorjani, M. (2018). Astaxanthin: a mechanistic review on its biological activities and health benefits. *Pharmacological Research*, **136**, 1–20.

Khalid, N., Shu, G.F., Holland, B.J., Kobayashi, I., Nakajima, M. & Barrow, C.J. (2017). Formulation and characterization of O/W nanoemulsions encapsulating high concentration of astaxanthin. *Food Research International*, **102**, 364–371.

Khoo, K.S., Lee, S.Y., Ooi, C.W. *et al.* (2019). Recent advances in biorefinery of astaxanthin from *Haematococcus pluvialis*. *Bioresource Technology*, **288**, 121606.

Kobayashi, M. & Sakamoto, Y. (1999). Singlet oxygen quenching ability of astaxanthin esters from the green alga *Haematococcus pluvialis*. *Biotechnology Letters*, **21**, 265–269.

Lee, J.S., Park, S.A., Chung, D. & Lee, H.G. (2011). Encapsulation of astaxanthin-rich Xanthophyllomyces dendrorhous for antioxidant delivery. *International Journal of Biological Macromolecules*, **49**, 268–273.

Leong, M.H., Tan, C.P. & Nyam, K.L. (2016). Effects of accelerated storage on the quality of kenaf seed oil in chitosan-coated high Methoxyl pectin-alginate microcapsules. *Journal of Food Science*, **81**, C2367–C2372.

Lin, S.F., Chen, Y.C., Chen, R.N. *et al.* (2016). Improving the stability of astaxanthin by microencapsulation in calcium alginate beads. *PLoS One*, **11**, 1–10.

Liu, S., Low, N.H. & Nickerson, M.T. (2010). Entrapment of flaxseed oil within gelatin-gum Arabic capsules. *Journal of the American Oil Chemists Society*, **87**, 809–815.

Liu, X.B. & Osawa, T. (2007). Cis astaxanthin and especially 9-cis astaxanthin exhibits a higher antioxidant activity in vitro compared to the all-trans isomer. *Biochemical and Biophysical Research Communications*, **357**, 187–193.

Madziva, H., Kailasapathy, K. & Phillips, M. (2005). Alginate-pectin microcapsules as a potential for folic acid delivery in foods. *Journal of Microencapsulation*, **22**, 343–351.

McNulty, H.P., Byun, J., Lockwood, S.F., Jacob, R.F. & Mason, R.P. (2007). Differential effects of carotenoids on lipid peroxidation due to membrane interactions: X-ray diffraction analysis. *Biochimica et Biophysica Acta-Biomembranes*, **1768**, 167–174.

Menin, A., Zanoni, F., Vakarelova, M. *et al.* (2018). Effects of microencapsulation by ionic gelation on the oxidative stability of flaxseed oil. *Food Chemistry*, **269**, 293–299.

Miki, W. (1991). Biological functions and activities of animal carotenoids. *Pure and Applied Chemistry*, **63**, 141–146.

Negash, Y.A., Amare, D.E., Bitew, B.D. & Dagne, H. (2019). Assessment of Quality of Edible Vegetable Oils Accessed in Gondar City, Northwest Ethiopia. *BMC Research Notes*. **12**, 1–5.

Niizawa, I., Espinaco, B.Y., Zorrilla, S.E. & Sihufe, G.A. (2019). Natural astaxanthin encapsulation: use of response surface methodology for the design of alginate beads. *International Journal of Biological Macromolecules*, **121**, 601–608. In this study, astaxanthin encapsulated in alginate beads was subjected to different storage conditions. Beads stored at 50 °C for 21 days showed le stability compared to our chitosan-shelled pectin beads stored at 65 °C, proving that pectin might contribute better to the protection of the carotenoid than alginate.

Pillay, V. & Fassihi, R. (1999a). In vitro release modulation from crosslinked pellets for site-specific drug delivery to the gastrointestinal tract—II. Physicochemical characterization of calcium-alginate, calcium-pectinate and calcium-alginate-pectinate pellets. *Journal of Controlled Release*, **59**, 243–256. This fundamental publication describes the gelling behaviour of alginate, pectin, and hybrid gels obtained by calcium cross-linking. The results show that alginate beads are characterized by better sphericity as a consequence of a faster setting of the gel and a more extended cross-linking. Our findings agree with the results of the Authors.

Pillay, V. & Fassihi, R. (1999b). In vitro release modulation from crosslinked pellets for site-specific drug delivery to the gastrointestinal tract. I. Comparison of pH-responsive drug release and associated kinetics. *Journal of Controlled Release*, **59**, 229–242.

Pu, J.N., Bankston, J.D. & Sathivel, S. (2011). Production of microencapsulated crawfish (*Procambarus clarkii*) astaxanthin in oil by spray drying technology. *Drying Technology*, **29**, 1150–1160.

Rodriguez-Ruiz, V., Salatti-Dorado, J.A., Barzegari, A. *et al.* (2018). Astaxanthin-loaded nanostructured lipid carriers for preservation of antioxidant activity. *Molecules*, **23**, 1–12.

Shah, M.M.R., Liang, Y.M., Cheng, J.J. & Daroch, M. (2016). Astaxanthin-producing green microalga *Haematococcus pluvialis*: from single Cellto high value commercia products. *Frontiers in Plant Science*, **7**, 1–28.

Shimidzu, N., Goto, M. & Miki, W. (1996). Carotenoids as singlet oxygen quenchers in marine organisms. *Fisheries Science*, **62**, 134–137.

Simat, V., Rathod, N.B., Cagalj, M., Hamed, I. & Mekinic, I.G. (2022). Astaxanthin from crustaceans and their byproducts: a bioactive metabolite candidate for therapeutic application. *Marine Drugs*, **20**, 1–22.

Taksima, T., Limpawattana, M. & Klaypradit, W. (2015). Astaxanthin encapsulated in beads using ultrasonic atomizer and application in yogurt as evaluated by consumer sensory profile. *LWT-Food Science and Technology*, **62**, 431–437.

Tonon, R.V., Brabet, C. & Hubinger, M.D. (2010). Anthocyanin stability and antioxidant activity of spray-dried acai (*Euterpe oleracea* Mart.) juice produced with different carrier agents. *Food Research International*, **43**, 907–914.

Vakarelova, M., Zanoni, F., Lardo, P. *et al.* (2017). Production of stable food-grade microencapsulated astaxanthin by vibrating nozzle technology. *Food Chemistry*, **221**, 289–295. In this publication, we describe the ionic gelation process used in the present study, employing for the first-time low-methoxyl pectin (LMP) as gelling polymer for the encapsulation of astaxanthin. In addition, we describe the better performance of LMP compared to alginate in retaining oil during the preparation of the beads.

Velasco, J., Dobarganes, C. & Marquez-Ruiz, G. (2003). Variables affecting lipid oxidation in dried microencapsulated oils. *Grasas Y Aceites*, **54**, 304–314.

Xie, D., Gong, M.Y., Wei, W. *et al.* (2019). Antarctic krill (*Euphausia superba*) oil: a comprehensive review of chemical composition, extraction technologies, health benefits, and current applications. *Comprehensive Reviews in Food Science and Food Safety*, **18**, 514–534.

Yang, L., Qiao, X., Gu, J.Y. *et al.* (2021). Influence of molecular structure of astaxanthin esters on their stability and bioavailability. *Food Chemistry*, **343**, 1–7.

Yi, J., Lam, T.I., Yokoyama, W., Cheng, L.W. & Zhong, F. (2015). Beta-carotene encapsulated in food protein nanoparticles reduces peroxyl radical oxidation in Caco-2 cells. *Food Hydrocolloids*, **43**, 31–40.

Zanoni, F., Vakarelova, M. & Zoccatelli, G. (2019). Development and characterization of astaxanthin-containing whey protein-based nanoparticles. *Marine Drugs*, **17**, 1–16.

Zhang, X.J., Yin, W.J., Qi, Y.K., Li, X.C., Zhang, W.J. & He, G.H. (2017). Microencapsulation of astaxanthin in alginate using modified emulsion technology: preparation, characterization, and cytostatic activity. *Canadian Journal of Chemical Engineering*, **95**, 412–419.

Zhao, X.Y., Liu, H.K., Zhang, X.W., Zhang, G.X. & Zhu, H.T. (2019). Astaxanthin from *Haematococcus pluvialis* microencapsulated by spray drying: characterization and antioxidant activity. *Journal of the American Oil Chemists Society*, **96**, 93–102.